

MAO–SIU SOLAR PHYSICS COLLABORATIONS

R.J. Rutten

Sterrekundig Instituut Utrecht, Postbus 80 000, NL 3508 TA, Utrecht, The Netherlands
e-mail: R.J.Rutten@astro.uu.nl

The Kiev–Utrecht collaboration in solar physics has a long history and a bright future. In this report I highlight some of our joint analyses in the past, discuss the general solar physics context as I see it at present, and describe exciting research challenges which fit the Kiev–Utrecht expertise and interests.

INTRODUCTION

The collaboration in solar physics between the MAO at Kiev and the SIU at Utrecht (presently the “Sterrekundig Instituut Utrecht”, previously “Sterrewacht Sonnenborgh”) started with E.A. Gurtovenko’s stay at Utrecht in 1972 and was subsequently continued by myself in a two-month visit to the MAO in 1980 when I started working with E.A. Gurtovenko, N.G. Shchukina, V.A. Sheminova and R.I. Kostik on various projects.

After my return to Utrecht, a formal cooperation was endorsed in an official agreement signed by Y.A. Yatskiv for the MAO and M. Kuperus for the SIU. This cooperation was explicitly mentioned, in fact as singular example, in subsequent versions of the “Program of the cultural and scientific cooperation between the USSR and the Netherlands”, the protocol to the USSR–Netherlands cultural exchange treaty.

A subsequent highlight was the IAU Symposium “*Solar Photosphere: Structure, Convection and Magnetic Fields*”, organized at my instigation by the solar group at MAO with J.-O. Stenflo as SOC chair. It was the first IAU Symposium on solar physics held in the Soviet Union and of exceptional quality. My sentence “we may be at a turning point in international relationships” on the last page of the proceedings (Stenflo 1990) became true quickly enough that it also became the last solar physics IAU Symposium ever held in the Soviet Union.

Since then, the collaborative MAO–SIU traffic reversed in direction. Half a dozen members of the solar group have been my guest at Utrecht, La Palma and even Sacramento Peak, with N.G. Shchukina and V.A. Sheminova visiting most regularly. The MAO’s solar-group contacts expanded to include Solanki’s group at Lindau (then the Max Planck Institute für Aeronomie, now the Max-Planck-Institut für Sonnensystemforschung) and the solar group at the Instituto de Astrofísica de Canarias on Tenerife (where E.V. Khomenko holds a postdoc at present). The MAO–SIU collaborations also continue to date; an ongoing joint analysis is reported by V.A. Sheminova elsewhere in this issue. Our present collaborations are funded by INTAS. In fact, S.M. Osipov and O.V. Andriyenko of the MAO solar group are missing this meeting because they are observing at the German Vacuum Tower Telescope on Tenerife as part of our INTAS collaboration.

MAO–SIU RESEARCH OVERVIEW

The following list itemizes the MAO–SIU publications, identifying them by the ADS bibliographic codes by which they are known at http://adsabs.harvard.edu/default_service.html. I added the authors and an indication of the topic. The full references are given in the reference list.

- 1974SoPh...37...43G Gurtovenko, Ratnikova, de Jager: *heights of formation*
- 1975SoPh...42...43G Gurtovenko, Ratnikova, de Jager: *heights of formation*
- 1976pmas.conf...331G Gurtovenko, de Jager, Lindenbergh, Rutten: *line broadening*
- 1982A&A...115..104R* Rutten, Kostik: *NLTE masking*
- 1985SvA...29...72G Gurtovenko, Sheminova, Rutten: *photospheric velocity field*
- 1990IAUS...138...29S Shchukina, Shcherbina, Rutten: *photosphere diagnostics*
- 1990IAUS...138...35G Gurtovenko, Kostik, Rutten: *oscillator strengths*

To appear in: “Astronomy in Ukraine - Past, Present and Future”, Eds. Peter Berczik and Olga Bolotina, Procs. MAO 60th Anniversary Conference, Kinematika and Fizika Nebesnyh Tel, in press. Preprint: <http://www.astro.uu.nl/~rutten/>

- 1990asos.conf...92G Gurtovenko, Kostik, Rutten: *oscillator strengths*
- 1990dysu.conf...260C Carlsson, Rutten, Shchukina: *Mg I 12 micron features*
- 1992csss...7...518C Carlsson, Rutten, Shchukina: *Mg I 12 micron features*
- 1992A&A...253...567C* Carlsson, Rutten, Shchukina: *Mg I 12 micron features*
- 1992A&A...265...237B Bruls, Rutten, Shchukina: *NLTE in alkali spectra*
- 1994csss...8...270C Carlsson, Rutten, Bruls, Shchukina: *NLTE Li I cool stars*
- 1994A&A...288...860C Carlsson, Rutten, Bruls, Shchukina: *NLTE Li I cool stars*
- 1995aapn.conf...399K Kostik, Shchukina, Rutten: *solar iron abundance*
- 1996A&A...305...325K Kostik, Shchukina, Rutten: *solar iron abundance*
- 2004A&A...???...???S Sheminova, Rutten, Rouppe van der Voort: *fluxtube modeling*

where the last one is obviously still in production – in fact, we are working on it during this meeting. In the next sections I briefly describe the two papers marked by an asterisk as examples of our past collaborations.

NLTE MASKING

In Rutten & Kostik (1982) Roman and I explained the success of the standard Holweger and Holweger-Müller models for the solar photosphere in explaining Fe I and Fe II line formation as due to “NLTE-masking”. Our analysis was based on the superb thesis on Fe I NLTE of Lites (1972), summarized by Athay & Lites (1972). We showed that if one adopts the HSRA-like model atmosphere used by Lites with his corresponding NLTE populations for Fe I and comparable NLTE populations for Fe II computed by Cram et al. (1980) to derive an empirical formation-temperature model from the computed iron lines in the same manner that Holweger applied to observed iron lines, one automatically ends up with a Holweger-like model. Figure 1 shows that the scheme works well throughout the optical spectrum. We therefore claimed that the HOLMUL model is a self-fulfilling prophecy, explaining most lines quite well assuming LTE because its derivation is based on such lines assuming LTE.

Figure 2 illustrates the physics. Most optical Fe I lines have LTE source functions in the photosphere but ultraviolet overionization causes joint opacity deficits for all Fe I levels. These cause the horizontal height-of-formation shifts in Fig. 1. The strongest lines have NLTE source function deficits from photon losses in the chromosphere, which cause the vertical offsets of the circles from the LITES model in Fig. 1 (line darkening, no central reversals). For Fe II the situation is the reverse: low Fe II levels have LTE populations because Fe II is the majority stage, but excited Fe II levels are overpopulated through overexcitation (“pumping”) in the Fe II resonance lines at yet shorter wavelengths (Cram et al. 1980). The Fe II lines therefore weaken through source function NLTE.

For steeper temperature gradients the Fe I opacity deficits and the Fe II source function enhancements increase due to larger ultraviolet $J_\nu > B_\nu$ excesses (where J_ν is the angle-averaged monochromatic intensity, B_ν the Planck function). The resulting Fe I and Fe II line depths remain about the same. HOLMUL-like model stratifications follow from LTE line fitting even if the actual temperature gradient is even steeper than in the LITES (or the HSRA) model.

Reversely, NLTE masking goes away if the actual photosphere possesses a temperature gradient as shallow as the HOLMUL model and the chromosphere is actually as cool as a RE model. This would be the case if the Lites and HSRA models are too steep. The issue hinges on the so-called ultraviolet line haze. This was first pointed out for sunspot modeling by Zwaan (1975, cf. Greve & Zwaan 1980) and taken up later by Avrett (1985) who included increasingly larger numbers of the millions of lines tabulated by Kurucz (URL <http://cfa-www.harvard.edu/amdata/ampdata/kurucz23/sekur.html>). Their effect is to reduce the ultraviolet $J_\nu > B_\nu$ excesses in the upper photosphere, so that the ultraviolet overionization diminishes, the bound-free opacities increase, and empirical continuum-fitting models become less steep. The resulting Harvard models, first tabulated in the Maltby et al. (1986) sunspot paper and later updated by Fontenla et al. (1993), run close to HOLMUL and BELLEA in the upper photosphere. The shallower temperature gradient produces a 200 K higher temperature minimum value at the onset of the chromospheric temperature rise. The presence of the latter maintains the need for source function departures in strong lines that do not show reversals. A hidden complexity is that also many of the line-haze lines possess reversals when computed in LTE. These are avoided in Avrett’s modeling by imposing an ad-hoc source function transition from pure absorption in deep layers to pure scattering above the temperature minimum. Overionization is neglected in the line haze opacities. Thus, the NLTE complexities affect the computation of the line haze which undoes them, an awkward inconsistency necessitating large-volume NLTE line-blanketing computation (Anderson 1989, cf. Anderson & Athay 1989).

The NLTE masking quandary resurfaces in modern modeling. Even if the the one-dimensional mean has a sufficiently flat temperature gradient to avoid $J_\nu > B_\nu$ overionization and overexcitation, actual stellar atmospheres must contain locations with steeper radial gradients. In simulations of solar and stellar granulation, spectral lines from such locations

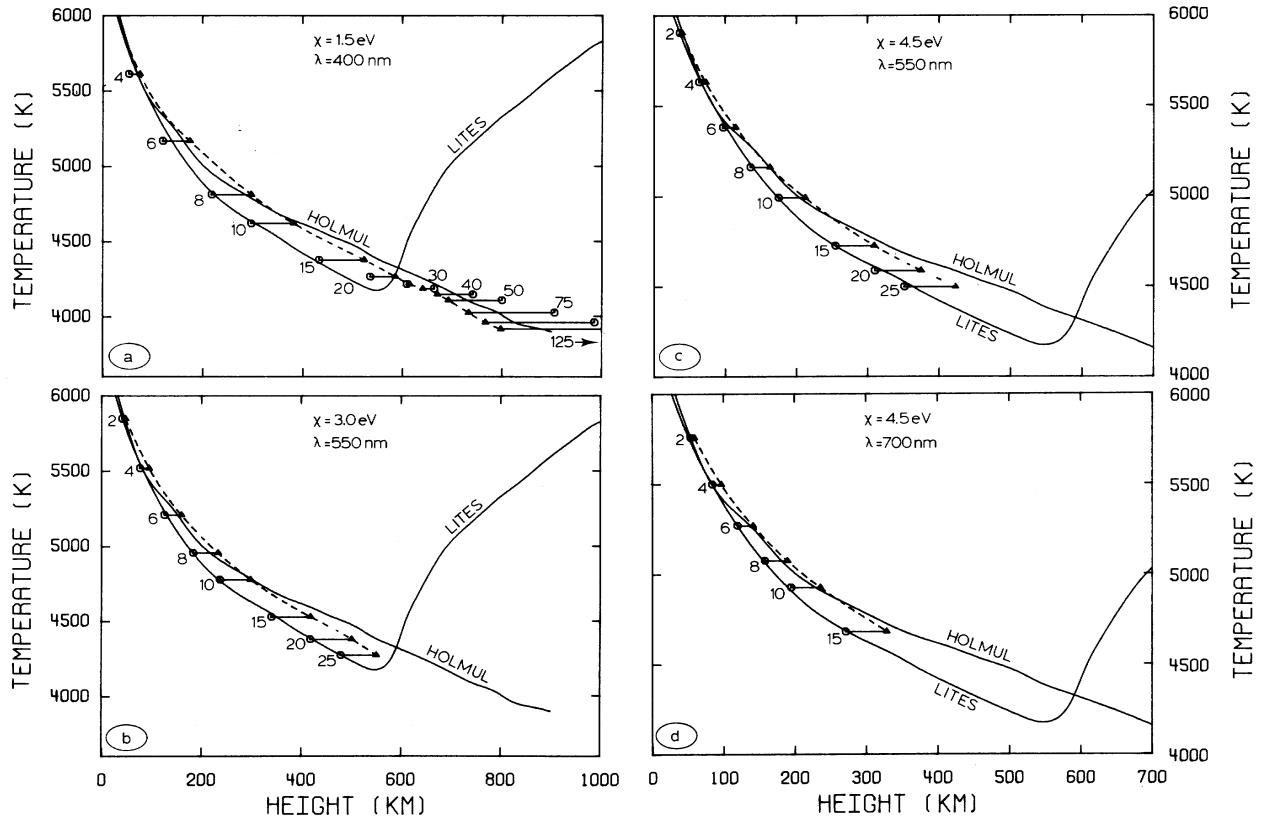


Figure 1. “NLTE masking” for Fe I lines at different excitation energy and wavelength. The circles denote line-center brightness temperatures of lines computed from Lites (1972) NLTE modeling, plotted at their height of formation. The numbers specify their equivalent width in pm. The triangles show the same brightness temperature but at the height of formation found when assuming LTE opacities. The dashed curves connecting the triangles simulate Holweger’s LTE model-building procedure. All four lie close to the actual HOLMUL model. This experiment shows that if the actual solar atmosphere obeys the LITES model with the concomitant NLTE departures, Holweger’s procedure inevitably produces a HOLMUL-like shallow-gradient model. Reversely, if the actual solar atmosphere obeys the HOLMUL model but one adopts a steeper-gradient model, one needs the concomitant $J_\nu > B_\nu$ NLTE departures to explain the observed lines. Thus, flat-LTE and steep-NLTE modeling explain Fe I lines about equally well. This quandary also holds for Fe II lines, for most other metals, for multi-component modeling, and for modern inversion methods. From Rutten & Kostik (1982).

with steep temperature gradients may be reproduced quite well from too shallow computed gradients by assuming LTE, or may be badly reproduced from correct gradients by NLTE modeling underestimating the ultraviolet line haze.

Similarly, spectral-line inversion codes assuming LTE, which basically automate Holweger’s modeling approach, may wrongly favor shallow-gradient models when based on LTE, or they may deliver too steep gradients from NLTE modeling when underestimating the ultraviolet line haze. It remains dangerous to rely on good correspondence between Fe I and Fe II line fitting as a proof of method validity since overionization and overexcitation may again affect the one and the other, respectively, with comparable results.

Both warnings come together when one-dimensional LTE inversions are gauged from LTE line formation computed from numerical simulations, as for example in the recent analysis by Allende Prieto et al. (2001) which combines the Holweger-like inversion method of Allende Prieto et al. (2000) with the granulation simulation of Asplund et al. (2000). At some height in the stellar atmosphere the apparent success of such inversions will at least partially be thanks to NLTE masking. So will apparent consistency between computed Fe I and Fe II line cores.

Mg I 12 MICRON EMISSION FEATURES

The most outspoken example of source function NLTE in the whole solar spectrum is the case of the two Mg I 12 micron emission features. The strongest one is shown in Fig. 6. They were discovered by Murcray et al. (1981), after they had

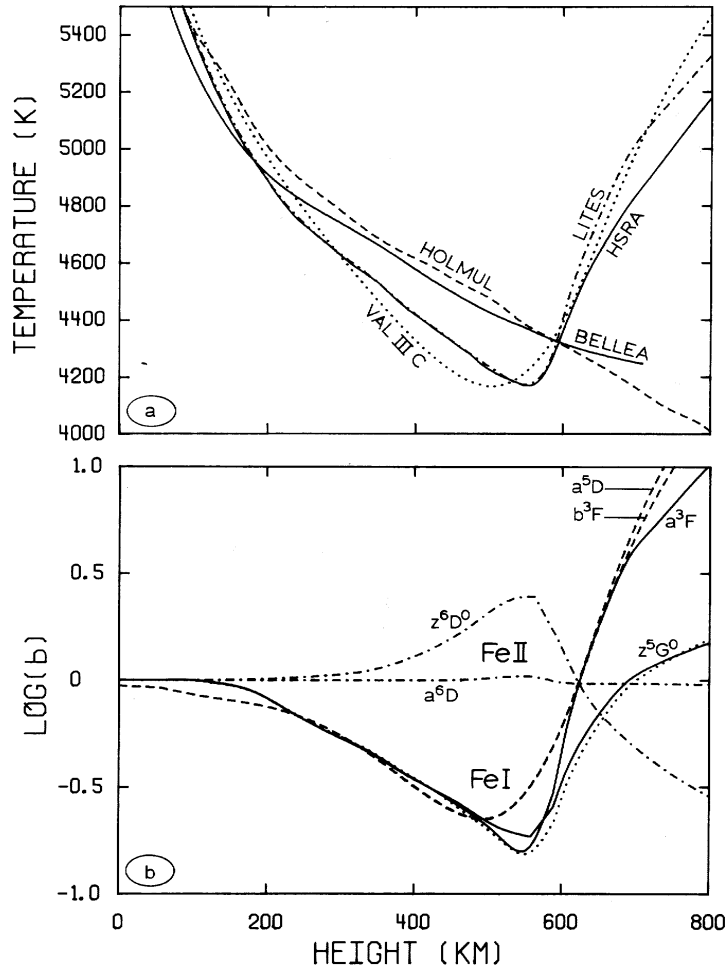


Figure 2. *Top*: selection of solar models. The HSRA (Gingerich et al. 1971) and VALIIC (Vernazza et al. 1981) are NLTE continuum-fitting models from Harvard. LITES is a modification of the HSRA by Lites (1972). BELLEA (Bell et al. 1976) is a theoretical RE model from Uppsala. HOLMUL (Holweger & Müller 1974) is an update of Holweger's (1967) model fitting Fe I lines assuming LTE. Notice the close resemblance of the latter two and the low-temperature upper photosphere of the HSRA-LITES and VALIIC models. *Bottom*: NLTE population departure coefficients b for representative levels of Fe I and Fe II for the LITES model. The joint dip of the Fe I curves comes from radiative overionization in the near ultraviolet. The peak of the Fe II z^6D^0 curve results from radiative overexcitation in Fe II resonance lines. The divergences at larger height, with higher-level curves dropping below lower-level curves, result from strong-line photon losses. Optical Fe I lines have LTE source functions but joint NLTE opacity depletion. Optical Fe II lines have LTE opacities but NLTE source function enhancements. Such departure behavior is characteristic for many metals when the upper-photosphere temperature gradient is steep enough to cause $J_\nu > B_\nu$ radiation excesses in the near ultraviolet. From Rutten & Kostik (1982).

earlier been noticed by Testerman and Brault and had even been hand-masked out of the spectrum atlas of Goldman et al. (1980) on the suspicion of being artifacts. Brault & Noyes (1983) were the first to study them in detail and showed that both lines contain strong emission peaks already at disk center. Subsequently, Chang & Noyes (1983) identified the lines as high-level transitions of Mg I.

Thanks to their long wavelength the lines have large Zeeman splitting, with fields of a few hundred Gauss already causing complete peak separation. Obviously, it is important to decide at which height the lines originate for diagnostic usage. The dilemma whether the emission peaks are photospheric or chromospheric was posed at the outset by Brault & Noyes (1983). It was the subject of a long and heated debate which is summarized in Carlsson, Rutten & Shchukina (1992). In that paper we identified the emission mechanism as being due to slight $b_u > b_l$ population divergence in

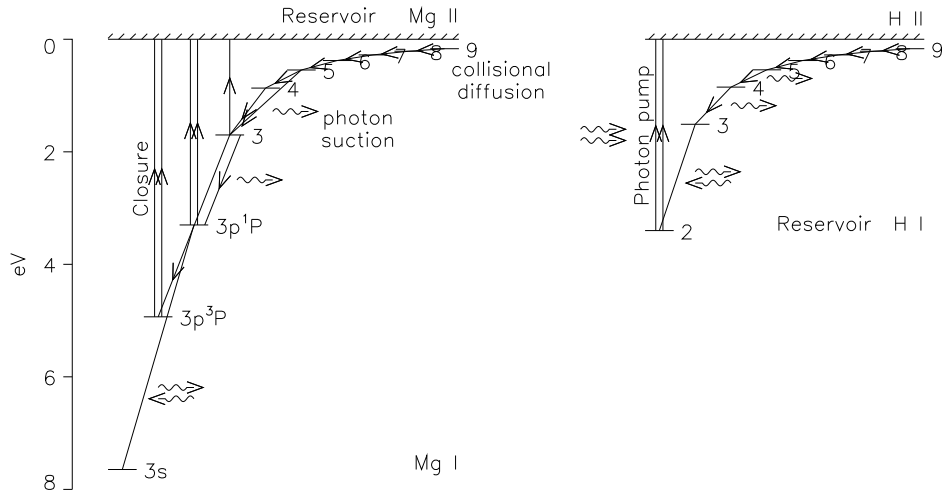


Figure 3. Schematic representations of the Mg I term diagram at left and the H I term diagram at right. Magnesium is predominantly singly ionized in the photosphere, so that the Mg II ground state constitutes the Mg LTE population reservoir. The lowest Mg I levels are too far from the continuum for ultraviolet overionization, which is most effective at 3–4 eV ionization energies ($\lambda = 400 - 300$ nm). The resonance transitions and other strong lines such as 3s–3p and the b lines are opaque and close to detailed balance. The main NLTE driver consists of a sequence of $\Delta n = 1$ and $\Delta n = 2$ lines at high l . These are strong in the laboratory sense, having large transition probabilities. The lines are sufficiently weak in the solar spectrum, due to their small Boltzmann populations, that they are thin in the middle photosphere. Their combined radiative losses cause photon suction: the photon losses in these lines are compensated from the population reservoir in the ion ground state, drawing replenishment population down until the the neutral-stage overpopulation is sufficiently large to balance the ionization equilibrium through photoionization closure. Thus, the line-driven suction produces overpopulation of levels 3 which with the superthermal radiation in their bound-free continua balances the ionization equilibrium. The schematic diagram at right for hydrogen illustrates the reverse case of an element which is predominantly neutral. For hydrogen, levels 1 and 2 constitute the LTE reservoir, with such strong coupling between the two through Ly α that detailed balance applies and level 1 does not play a role in the atmospheric regime to which this cartoon applies. The Balmer continuum has 3.4 eV ionization energy and feeds on superthermal radiation with $J_\nu > B_\nu$ from the deep photosphere. This pumping is strongly enhanced by photon suction in H α , as originally established by Auer & Mihalas (1969a, 1969b) in their landmark papers. See Wiersma et al. (2003) for a modern re-computation of their work, and study the final problem in Rutten (2000) for in-depth analysis of their results. From Rutten & Carlsson (1994).

the upper photosphere (we actually used an RE model without chromosphere). The divergence results from collisional cascade through high levels which maintains a diffusive recombination flow into lower levels that is driven by photon losses in strong lines and radiative overionization. This “photon suction” mechanism is illustrated in Figs. 3–6.

The resulting population divergence is only a few percent, but its effect on the emergent line profiles is large due to the b_u/b_l ratio of the NLTE upper- and lower-level population departure coefficients in the correction for stimulated emission in:

$$\frac{S_{\nu_0}^l}{B_{\nu_0}} = \frac{1 - e^{-h\nu_0/kT}}{(b_l/b_u) [1 - (b_u/b_l) e^{-h\nu_0/kT}]}, \quad (1)$$

implying source function enhancement over the Planck function when $(b_u/b_l) \exp(-h\nu_0/kT)$ goes down to unity. Figure 5 illustrates this, showing that the source function blows up to large values before it goes negative in the lasing regime. Figure 6 finally shows the result of our modeling. The reproduction of the observations is excellent. Since no ad-hoc fitting parameter was used in our modeling, the very good agreement implies that the Rydberg levels of Mg I in the solar photosphere behave rather the same as those in our computer. Our modeling proved unequivocally that the Mg I emission features originate in the photosphere.

The Mg I 12 micron lines have since been used to identify superpenumbrae around sunspots (Bruls et al. 1995), but more extensive application as sensitive Zeeman diagnostics awaits higher-resolution infrared observing capability.

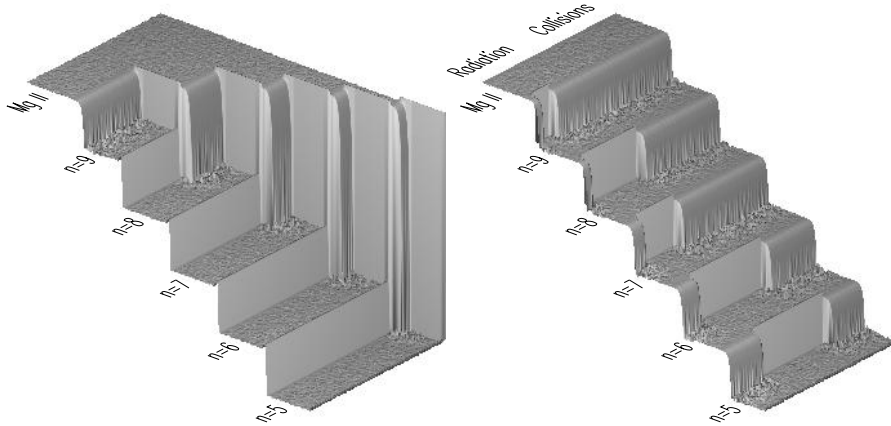


Figure 4. Cartoons illustrating the collisional nature of the NLTE cause of the Mg I 12-micron emission features. The replenishment population flow from the continuum reservoir comes down primarily along the Rydberg ladder of close-lying high levels. It is collisionally dominated along its top. The lefthand waterfalls illustrate that most of the replenishing recombination enters at the $n = 9$ top of the Mg I model atom used by Carlsson et al. (1992). The Mg II—9 waterfall would undoubtedly be split into recombination into yet higher steps if the atomic model accommodated these, but such splitting would not affect the 7–6 step which harbors the $12 \mu\text{m}$ lines. The cascade at right shows the split between net collisional and radiative deexcitation along $\Delta n = 1$ steps. Collisions already dominate the 7–6 transition, and gain even more higher up. From Rutten & Carlsson (1994).

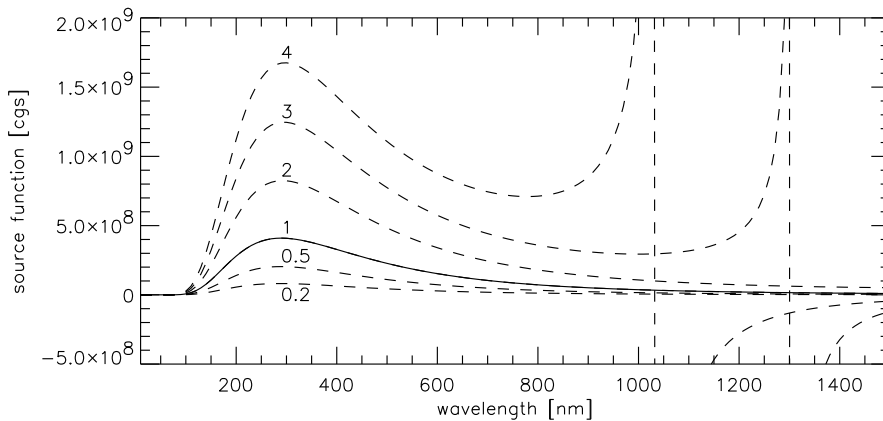


Figure 5. Wavelength variation of the line source function for $T = 10\,000\text{ K}$ and the specified ratios b_u/b_l , in cgs units with $\Delta\lambda = 1\text{ nm}$. The NLTE source function scales with the Planck function (solid curve) in the Wien part at left, but reaches the laser regime for large b_u/b_l in the Rayleigh-Jeans part at right. From Rutten (2000).

SOLAR PHYSICS CONTEXT

Solar physics presently experiences a marked renaissance, following a period in which analytical and “cartoon” modeling became inadequate to cope with the actual complexities imposed by solar magnetism. The advent of large-scale computing and sophisticated numerical modeling has turned the tide: solar physics is now a field in which observed phenomena are addressed through increasingly realistic numerical simulations. These permit experimentation to find out why the Sun supplies such rich astrophysics displays to inquisitive terrestrials. These advances also define an urgent need for better observations, with much higher resolution, over much longer duration, and with much better diagnostic quantification than sufficed before.

Fortunately, observational solar physics is currently undergoing a matching revolution through the advent of wavefront

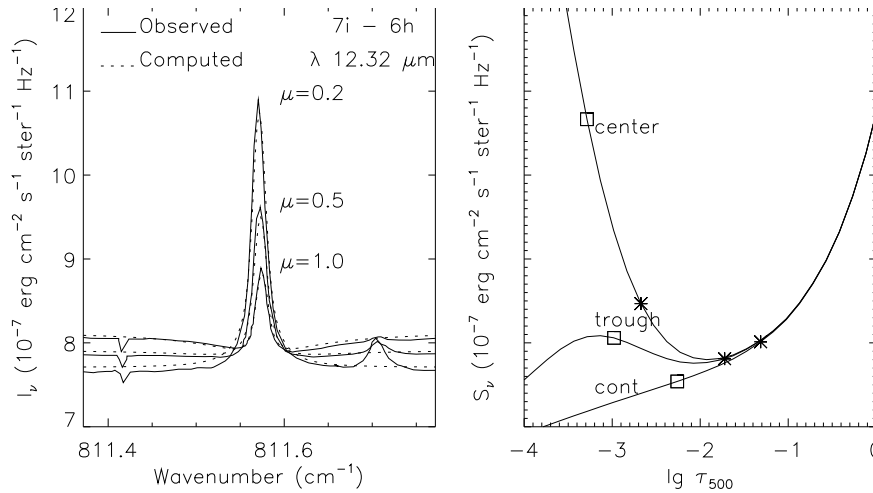


Figure 6. Profiles and source functions of the Mg I 12.32 μm line ($7i - 6h$). *Left*: observed and computed profiles on absolute intensity scales, for the three viewing angles θ indicated by $\mu = \cos \theta$. The observed profiles are based on Brault & Noyes (1983). *Right*: computed source functions, for line center, an inner-wing wavelength (“trough”) and the continuum. Average formation heights are specified by squares for $\mu = 0.2$, stars for $\mu = 1$. These two panels demonstrate the mapping of the source function at right into the profiles at left. The steep outward rise of the line-center source function results from small b_u/b_l population excess shown in Carlsson et al. (1992). From Rutten & Carlsson (1994).

restoration which removes the detrimental effects of turbulence in the Earth’s atmosphere on telescopic image quality. This dramatic revolution is another prime example of the general computer revolution in the physical sciences: the increase in processing speed now enables near-perfect wavefront restoration both through real-time adaptive optics technology and through post-detection image processing. Both techniques are similar between solar imaging and nighttime astronomy, but not identical because the Sun is an extended low-contrast object on our sky rather than a weak point source. Solar wavefront restoration requires special techniques to beat low signal-to-noise ratios.

The prime example of these new observing capabilities is the American project to build a four-meter Advanced Technology Solar Telescope (URL <http://atst.nso.edu>) which will combine a four-meter obstruction-free aperture with high-order adaptive optics and elaborate post-focus instrumentation. This 170-million dollar project is intended in particular to elucidate the role of solar magnetism in setting the structure and dynamics of the solar atmosphere.

There is threefold motivation to study solar magnetism: (i) – astrophysics, employing the sun as “Rosetta Stone” to investigate conditions and processes that are commonplace in the wider universe but are seen close-up only in the sun; (ii) – magnetohydrodynamics and plasma physics, with the sun a relatively close-by “cosmic laboratory” that adds length, time, temperature and density regimes not attainable in earth-based laboratories such as Tokamaks; (iii) – the solar modulation of the human environment through “space weather”, *i.e.* the combined effects of solar cosmic-ray modulation, solar particle storms, and solar irradiance variations that affect our terrestrial neighborhood and possibly climate on both short and long time scales. The latter interests make solar physics directly socially relevant, and a currently booming industry in the USA.

Magnetism defines and controls the complex interactions between the solar photosphere and the outer solar atmosphere. Magnetic fields break through the solar surface in a hierarchy of magnetic elements ranging from Earth-sized sunspots down to the slender fluxtubes that at high resolution appear as tiny network bright points. These magnetic elements are organized in intricate, continuously evolving patterns that constitute solar activity, control the structure and dynamics of the solar corona and the solar wind, and affect the extended heliosphere including the near-earth environment and possibly the terrestrial climate.

The patterning and evolution of solar magnetic fields are dictated by the subsurface dynamo and convective flows but in turn they dictate the structure, dynamics, and heating of the outer atmosphere. This switch in field role occurs in the optically observable photosphere–chromosphere regime, so that ground-based imaging permits charting the magnetic “footpoint” topology and dynamics.

The footpoint “fluxtubes” are imaged sharpest at the base of the solar atmosphere (photosphere) when observed in the Fraunhofer G-band (a cluster of molecular CH lines around $\lambda = 430.5$ nm). These magnetic flux ropes bundle in clusters that can be traced up to the chromosphere through imaging in the Ca II H&K lines. and then spread out in magnetic

fibrils seen in the HI Balmer- α line. In the solar corona the field is structured in extended loops that are observable with space-based ultraviolet and X-ray imaging (presently the SOHO, TRACE and RHESSI missions, in future the Solar-B, SDO and Solar Orbiter missions).



Figure 7. The Dutch Open Telescope at the Spanish Observatorio del Roque de los Muchachos of the Instituto de Astrofísica de Canarias on La Palma. Left: 15-m high open tower with telescope. North is to the right. The triangular geometry of the tower stilts is such that the platform can only move laterally, without tilt, so that the telescope (focused at infinity) shows no image motion even in strong wind buffeting. Right: close-up of the telescope. The mirror diameter is 45 cm but the mount can accommodate a 140 cm mirror. The flexible tubes serve for air suction around prime focus. The reflective heat stop is water-cooled. The boxes at the top contain the multi-wavelength imaging system with six CCD cameras and a phase-diverse focus monitor. Glass fiber links to the Swedish telescope building housing the Swedish 1-m Solar Telescope (SST) transport both the control signals and the image streams. The new DOT Speckle Processor is placed in the nearby building housing the Carlsberg Meridian Telescope, also connected via glass fibers. The SST uses adaptive optics for wavefront restoration and is equipped with a spectrometer and will soon also furnish spectropolarimetry. Since the DOT and SST share identical seeing, co-pointing is a logical strategy to combine spectral diagnostics with wide-field imaging, and will frequently be scheduled the coming years. Photographs by R.H. Hammerschlag.

FUTURE SOLAR PHYSICS AT THE SIU

My solar physics group at the SIU is presently largely devoted to putting a new optical solar telescope into full operation and analyzing the superb image sequences which it produces. Our Dutch Open Telescope (DOT) on La Palma is an innovative solar telescope which successfully achieves sustained high-resolution tomographic imaging of the solar atmosphere. It reaches very high image-sequence quality by combining an open design at a superior wind-swept site (Fig. 7)

Table 1. DOT filter specification.

designation	λ (Å)	width (Å)	type	tuning
blue continuum	4320	6	interference	fixed
red continuum	6540	3	interference	tiltable
G band	4305	10	interference	fixed
Ca II H	3968	1.35	interference	tiltable
H α	6563	0.25	Lyot	tunable
Ba II	4554	0.08	Lyot	tunable

with elaborate image processing using speckle reconstruction. Details are given in Rutten et al. (2004) and on the DOT website at URL <http://dot.astro.uu.nl>.

The DOT is open and mounted equatorially on a 15 m high open tower in order to exploit the strong La Palma trade wind. The latter flushes the 45 cm primary mirror and the telescope interior, and so inhibits internal turbulence. The parallactic mount is exceedingly stiff to avoid wind-induced telescope shake. An elaborate multi-camera speckle image acquisition system collects and stores up to 1.8 Terabyte of speckle data per observing day. A sophisticated 70-processor computer farm is being installed to achieve full speckle reconstruction of such large data sets within the next day. By working in the image plane, this technique permits restoration of the full field of view to the 0.2 arcsec diffraction limit defined by the DOT aperture.

The DOT was designed and built by Robert H. Hammerschlag with coworkers at Utrecht and the university workshops at Delft and Utrecht. The open concept was revolutionary. So far, all high-resolution solar telescopes use evacuation to avoid internal turbulence caused by internal solar heating. The open DOT instead relies on telescope flushing by the strong laminar trade winds which make La Palma a world-class solar site. The DOT's successful demonstration of this principle spawned a wave of new large-telescope projects elsewhere¹.

The DOT is presently being equipped with multi-wavelength optics feeding six synchronously-operated cameras with dual fiber-optic links to the control and data-acquisition computers in the Swedish telescope building. The wavelength and filter characteristics are given in Table 1. The first five are working. The superb birefringent tunable Lyot filter for Ba II 455.4 nm, on loan from the Institute of Solar-Terrestrial Physics at Irkutsk (Sütterlin et al. 2001), will be installed the coming spring. The six synchronous channels together constitute tomographic sampling of the solar atmosphere from the deep photosphere (continua and G band) through the high photosphere (Ba II Dopplergrams and magnetograms, extended wing blue wing of Ca II H), and the low chromosphere (Ca II H center) to the high chromosphere and low transition region (H α). Complementary EUV and X-ray observation from space, in particular the TRACE and future SDO missions, add coronal topology and dynamics.

A key topic for such high-resolution topology mapping is the nature of the magnetic coupling between the high-beta and low-beta parts of the solar atmosphere. It is easy to claim paradigmatically that photospheric fluxtubes expand into magnetic canopies and combine into coronal loops, but this picture is far too schematic. The actual “canopy” (which should be defined as the $\beta = 1$ manifold) and the actual “transition region” (which should be defined as the 50% hydrogen ionization manifold) are highly folded, finely structured, and highly dynamic surfaces, not obeying “layer” or “shell” geometry at all. Mapping actual canopy and transition region topologies and dynamics is an essential step towards understanding the magnetic coupling between the $\beta > 1$ solar interior and photosphere, the $\beta < 1$ upper chromosphere and low corona, and the magnetically structured outer corona and wind.

FUTURE SOLAR PHYSICS AT THE MAO

Solar physics at the MAO is making the same transition that I have made with my students at the SIU: from spectroscopy concentrating on solar line formation to the application of optical (and infrared) diagnostics to study dynamic phenomena and magnetism in the solar atmosphere. It is not for me to set directions for the solar physics group at the MAO, but it is easy to point out a major MAO strength. This is precisely the radiative transfer expertise that the MAO built up starting

¹The new open telescopes break the 1-m limit imposed on vacuum windows and refractor objectives by glass technology. The newly rebuilt Swedish 1-m Solar Telescope (SST) on La Palma, from whose building the DOT is operated, is at 1-m the largest feasible refractor. It pioneers in being the first solar telescope reaching 1-m resolution (0.1'' in the visible; see Scharmer et al. 2002). The SST uses adaptive optics to correct the seeing, a complementary technique to the DOT's speckle reconstruction which works in the pupil plane instead of the image plane. AO works in real time, but optimally only for the central isoplanatic patch. With the DSP in place at the DOT, tandem SST-DOT operation is likely to be scheduled very frequently, with the SST furnishing 0.1'' spectropolarimetry and the DOT tomographic context at 0.2''. All other large-telescope projects concern open reflectors. They are, in brief, the German 1.5 m GREGOR for Tenerife (first light around 2005), the 1.6 m New Solar Telescope for Big Bear Solar Observatory (2006?), the 1 meter Indian MAST for Udaipur Solar Observatory (proposed), and the 4 meter American ATST (first light 2012?). They mostly target AO spectropolarimetry. The DOT team assists actively in all projects (guider and turret hardware of the SST; GREGOR dome fabrication; MAST, NST and ATST designs). An upgrade of the DOT to 1.4-m aperture is feasible but yet unfunded.

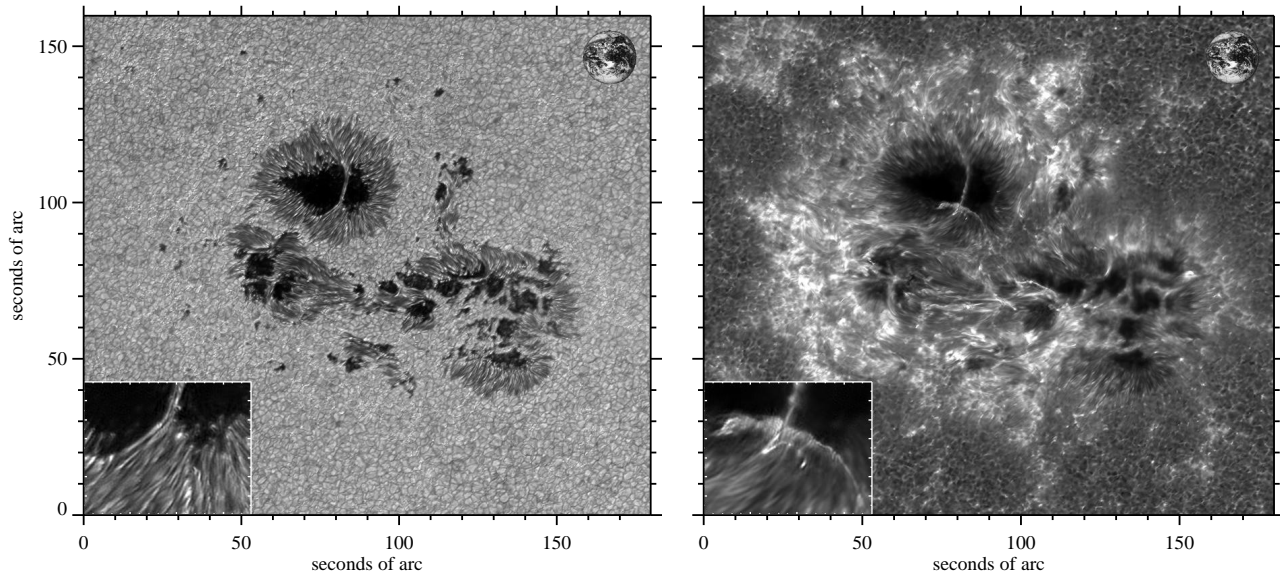


Figure 8. Co-spatial and synchronous speckle-reconstructed DOT image mosaics of solar active region AR10375 taken on June 6, 2003. The Earth inserts indicate the geometric scale. The lower-left inserts show a magnified part of the largest spot. The lefthand image samples the solar photosphere in the Fraunhofer G band, consisting of molecular CH lines around 430.5 nm. It shows a large active region with multiple sunspots, surrounded by solar granulation and tiny bright magnetic elements within the intergranular lanes. The righthand image samples the overlying chromosphere about 500 km higher up in the strong Ca II H line (396.8 nm). The striking differences between the two scenes demonstrate substantial changes in the magnetic field topology between the photosphere and chromosphere. Thanks to the speckle reconstruction the angular resolution in the original images (see insets) is close to the 0.2 arcsec DOT diffraction limit over the whole field. The DOT excels in producing such sharp large-field tomographic imagery as movies with exceptional quality homogeneity over long duration. Images provided by P. Sütterlin.

with the efforts of E.A. Gurtovenko. There are not many research groups that really understand spectral line formation to the full depth of its NLTE intricacies. At many places the research emphasis lies on image processing and movie making. These have become highly sophisticated industries, which is certainly a necessity in solar physics. Static plane-parallel modeling is very much a tractability simplification of the past. However, movie making and movie analysis is not enough since any solar image sequence is based on a specific spectral diagnostic that needs to be understood in depth. There are only a few diagnostics for which simple LTE modeling is a fair strategy. The wings of Ca II H & K and the infrared CO lines come to mind, but even these pose intricate complexities the moment one starts wondering about dynamical phenomena and time scales. A sound background in solar line formation including a good grasp of complex phenomena such as *e.g.* NLTE masking, photon suction, photon pumping, Zanstra recombination, partial frequency redistribution, Zeeman broadening and Hanle depolarization is a great asset.

FUTURE SIU-MAO COLLABORATIONS

As I have sketched above, my Utrecht group in solar physics concentrates at present on our efforts to get the Dutch Open Telescope in full production. The timing of this meeting coincides with a transition from DOT development to DOT usage. From next spring onward, with our tomography system complete and our speckle processor ready to process eight hours of continuous six-camera runs every day, we aim to observe frequently, often co-pointing with other telescopes, in particular the SST. There will be a flood of high-resolution data combining DOT tomography with SST spectropolarimetry, both at 0.2 arcsec resolution and reaching that fairly frequently during sequences of one to multiple hours duration. There will be a shortage of astrophysicists with the expertise needed for full harvesting. New MAO-SIU collaborations may well aim to mine this rich data supply. It is easy to formulate a research topic list:

- *solar wave dynamics*: network and internetwork oscillations, internal gravity waves, umbral flashes, wave excitation and mode conversion in magnetic elements;
- *solar magnetism*: magnetic-element emergence, fluxtube collapse, fluxtube dynamics, magnetic carpet topology and evolution, sunspot structure and dynamics;

- *canopy transitions*: wave penetration and heating, moss structure and dynamics, magnetic tube-loop coupling, spicule physics.

CONCLUSION

Let me finish by remarking that Utrecht astronomy is 300 years older than the MAO. The MAO is even younger than I am myself. I am glad to have witnessed and to even have participated in the opening of MAO solar physics to the West and vice-versa, but what counts rather more is what the future will bring. There are excellent solar physicists at MAO also in the young generation, and also at Utrecht bright students still embark on science careers. The Sun offers a host of exciting problems for them to work on. In particular, solar magnetism offers much fascinating science for decades to come - so far, we have barely scratched the surface of this rich source of astrophysics. I sincerely hope that the economical climate in the Ukraine will permit Ukrainian solar physics to not only maintain its high quality but even expand exploiting its excellent international relations.

ACKNOWLEDGEMENTS

I thank the organizers of the MAO-60 Conference for inviting me to this pleasant meeting. I am much indebted to Roman I. Kostik, Natalya G. Shchukina, Elena V. Khomenko and Valentina A. Sheminova for much hospitality during my stay in Kiev. The MAO–SIU collaboration is supported by INTAS under Contract 00-00084.

*

References

- Allende Prieto C., Barklem P. S., Asplund M., Ruiz Cobo B., 2001, *ApJ* 558, 830
Allende Prieto C., García López R. J., Lambert D. L., Ruiz Cobo B., 2000, *ApJ* 528, 885
Anderson L. S., 1989, *ApJ* 339, 558
Anderson L. S., Athay R. G., 1989, *ApJ* 336, 1089
Asplund M., Nordlund Å., Trampedach R., Allende Prieto C., Stein R. F., 2000, *A&A* 359, 729
Athay R. G., Lites B. W., 1972, *ApJ* 176, 809
Auer L. H., Mihalas D., 1969a, *ApJ* 156, 157
Auer L. H., Mihalas D., 1969b, *ApJ* 156, 681
Avrett E. H., 1985, in B. W. Lites (ed.), *Chromospheric Diagnostics and Modeling*, National Solar Observatory Summer Conference, Sacramento Peak Observatory, Sunspot, p. 67
Bell R. A., Eriksson K., Gustafsson B., Nordlund Å., 1976, *A&AS* 23, 37
Brault J., Noyes R., 1983, *ApJ* 269, L61
Bruls J. H. M. J., Rutten R. J., Shchukina N. G., 1992, *A&A* 265, 237
Bruls J. H. M. J., Solanki S. K., Rutten R. J., Carlsson M., 1995, *A&A* 293, 225
Carlsson M., Rutten R. J., Bruls J. H. M. J., Shchukina N. G., 1994, *A&A* 288, 860
Carlsson M., Rutten R. J., Bruls J. H. M. J., Shchukina N. G., 1994, in J. P. Caillault (ed.), *Cool Stars, Stellar Systems, and the Sun*, Proc. Eighth Cambridge Workshop, ASP Conf. Ser., Vol. 64, p. 270
Carlsson M., Rutten R. J., Shchukina N. G., 1990, in L. Deszö (ed.), *The Dynamic Sun*, Proc. EPS 6th European Solar Meeting, Publ. Debrecen Heliophysical Observatory 7, Debrecen, p. 260
Carlsson M., Rutten R. J., Shchukina N. G., 1992, in M. S. Giampapa, J. A. Bookbinder (eds.), *Cool Stars, Stellar Systems, and the Sun*, Proc. Seventh Cambridge Workshop, ASP Conf. Ser., Vol. 26, p. 518
Carlsson M., Rutten R. J., Shchukina N. G., 1992, *A&A* 253, 567
Chang E. S., Noyes R. W., 1983, *ApJ* 275, L11
Cram L. E., Rutten R. J., Lites B. W., 1980, *ApJ* 241, 374
Fontenla J. M., Avrett E. H., Loeser R., 1993, *ApJ* 406, 319
Gingerich O., Noyes R. W., Kalkofen W., Cuny Y., 1971, *Sol. Phys.* 18, 347
Goldman A., Blatherwick R. D., Murcray F., van Allen J. W., Bradford C. M., Cook G. R., Murcray D. G., 1980, *New Atlas of Infrared Solar Spectra*. Volume I: Line Positions and Identifications, Volume II: The Spectra, Department of Physics, University of Denver
Greve A., Zwaan C., 1980, *A&A* 90, 239
Gurtovenko E., Ratnikova V., de Jager C., 1974, *Sol. Phys.* 37, 43
Gurtovenko E., Ratnikova V., de Jager C., 1975, *Sol. Phys.* 42, 43
Gurtovenko E. A., de Jager C., Lindenbergh A., Rutten R. J., 1976, in R. Cayrel, M. Steinberg (eds.), *Physique des mouvements dans les atmosphères stellaires*, Coll. No. 250, Centre Nat. de la Recherche Scientifique, Paris, p. 331

- Gurtoenko E. A., Kostik R. I., Rutten R. J., 1990a, in J.-O. Stenflo (ed.), *The Solar Photosphere: Structure, Convection and Magnetic Fields*, IAU Symp. 138 (Kiev), Kluwer, Dordrecht, p. 35
- Gurtoenko E. A., Kostik R. I., Rutten R. J., 1990b, in J. E. Hansen (ed.), *Atomic Spectra and Oscillator Strengths for Astrophysics and Fusion Research*, Royal Neth. Acad. Sciences, *Verhandelingen Afd. Natuurkunde, Eerste Reeks* **33**, North-Holland, Amsterdam, p. 92
- Gurtoenko E. A., Sheminova V. A., Rutten R. J., 1985, *Soviet Astronomy* **29**, 72
- Holweger H., 1967, *Zeitschr. f. Astrophysik* **65**, 365
- Holweger H., Müller E. A., 1974, *Sol. Phys.* **39**, 19
- Kostik R. I., Shchukina N. G., Rutten R. J., 1995, in S. J. Adelman, W. L. Wiese (eds.), *Astrophysical applications of powerful new databases*, IAU, ASP Conf. Ser., Vol. 78, p. 399
- Kostik R. I., Shchukina N. G., Rutten R. J., 1996, *A&A* **305**, 325
- Lites B. W., 1972, *Observation and Analysis of the Solar Neutral Iron Spectrum*, NCAR Cooperative Thesis No. 28, High Altitude Observatory, Boulder
- Maltby P., Avrett E. H., Carlsson M., Kjeldseth-Moe O., Kurucz R. L., Loeser R., 1986, *ApJ* **306**, 284
- Murcray F. J., Goldman A., Murcray F. H., Bradford C. M., Murcray D. G., Coffey M. T., Mankin W. G., 1981, *ApJ* **247**, L97
- Rutten R. J., 2000, *Radiative Transfer in Stellar Atmospheres*, Lecture Notes Utrecht University, 7th WWW Edition, <http://www.astro.uu.nl/~rutten>
- Rutten R. J., Carlsson M., 1994, in D. M. Rabin, J. T. Jefferies, C. Lindsey (eds.), *Infrared Solar Physics*, Proc. Symp. 154 IAU (Tucson), Kluwer, Dordrecht, p. 309
- Rutten R. J., Hammerschlag R. H., Bettonvil F. C. M., Sütterlin P., de Wijn A. G., 2004, *A&A* **413**, 1183
- Rutten R. J., Kostik R. I., 1982, *A&A* **115**, 104
- Scharmer G. B., Gudiksen B. V., Kiselman D., Löfdahl M. G., Rouppe van der Voort L. H. M., 2002, *Nature* **420**, 151
- Shchukina N. G., Shcherbina T. G., Rutten R. J., 1990, in J.-O. Stenflo (ed.), *Solar Photosphere: Structure, Convection and Magnetic Fields*, IAU Symp. 138 (Kiev), Kluwer, Dordrecht, p. 29
- Stenflo J.-O. (ed.), 1990, *Solar Photosphere: Structure, Convection, and Magnetic Fields*, Proc. IAU Symp. 138 (Kiev), Kluwer, Dordrecht
- Sütterlin P., Rutten R. J., Skomorovsky V. I., 2001, *A&A* **378**, 251
- Vernazza J. E., Avrett E. H., Loeser R., 1981, *ApJS* **45**, 635
- Wiersma J., Rutten R. J., Lanz T., 2003, in I. Hubeny, D. Mihalas, K. Werner (eds.), *Stellar Atmosphere Modeling*, Procs. Tübingen Workshop, ASP Conf. Ser., Vol. 288, p. 130
- Zwaan C., 1975, *Sol. Phys.* **45**, 115